

# Computational Fluid Dynamic (CFD) Analysis of Tray Dryer Performance for Turmeric Rhizome Drying

Duc T. Le<sup>a,b</sup>, Nhu V.P Le<sup>a,b</sup>, Yen H.P Duong<sup>a,b</sup>, Tan M. Le<sup>a,b</sup>, Viet T. Tran<sup>a,b,\*</sup>

<sup>a</sup>Faculty of Chemical Engineering, Ho Chi Minh City University of Technology (HCMUT), 268 Ly Thuong Kiet Street, Ho Chi Minh City, Vietnam

<sup>b</sup>Vietnam National University Ho Chi Minh City (VNU-HCM), Linh Trung ward, Thu Duc District, Ho Chi Minh City, Viet Nam  
[trantanviet@hcmut.edu.vn](mailto:trantanviet@hcmut.edu.vn)

In this research, Computational Fluid Dynamics (CFD) is employed to simulate the distribution of velocity, temperature, and mass fraction of water vapor in moist air and the evaporation rate of drying material within a drying chamber. These simulations are grounded in the application of conservation principles for mass, momentum, and energy. Experiments were conducted at building H3 in HCMUT at the Di An Campus to measure velocity and temperature at various locations within the drying chamber and the mass of dried turmeric rhizome. To model the drying process of turmeric rhizome in a tray dryer, the CFD software ANSYS Fluent was utilized for 3D modeling. Various models, such as the standard k-epsilon turbulence model and the species model used in conjunction with the transient solver, were employed to analyze the distribution of velocity, temperature, the mass fraction of water vapor in moist air, and the evaporation rate of the drying material within the tray dryer over 8000 seconds with a drying agent at 50 °C. The simulation results for the evaporation rate of the drying material and drying temperatures were compared to experimental data and found to be in excellent agreement. This was indicated by R<sup>2</sup> values of 1, 0.99, and 0.97 for the three drying stages. Consequently, simulation can serve as a viable option for studying drying mechanisms and mitigating certain limitations associated with conducting experiments.

## 1. Introduction

Turmeric (*Curcuma longa*) is a flowering plant species belonging to the ginger family, valued for its wide range of uses in cooking and medicine in Vietnam. This species is widely cultivated in Lao Cai, Lang Son, Vinh Phuc, Hung Yen, Nghe An, and the Central Highlands, yielding substantial profits for farmers (Nguyen et al., 2020). Given the large production volumes, it is crucial to provide effective preservation methods for turmeric rhizomes to maintain their quality for economic purposes. Although there are many ways to preserve turmeric rhizomes, drying is the oldest method for removing moisture content, which creates a suitable environment for bacteria growth. One of the primary drying methods used for turmeric rhizomes is convection drying, which is known for its efficiency and speed. Investigating the physicochemical changes during this drying process and developing novel strategies to optimize energy consumption to provide better-dried turmeric quality is becoming increasingly important and highly encouraged. However, these advancements require significant time and costly laboratory and experimental efforts. Additionally, drying is a complex process due to the changes in moisture evaporation for the airflow characteristics and temperature distribution within the drying chamber, which are not easily visualized in practice. To overcome this problem, Computational Fluid Dynamics (CFD) can analyze the spatial distribution of relevant parameters within the drying chamber (Getahun et al., 2021).

Recent research has utilized CFD simulations to investigate convection drying. Previous studies have determined the optimal design for constructing a new drying chamber using CFD tools (Misha et al., 2013). Optimal conditions for drying mushrooms in tray dryers have been explored through CFD-based models (Nadew et al., 2023). Additionally, 3D CFD simulations have proven effective in identifying the most efficient drying times in solar greenhouse dryers (Duong et al., 2021). The process of almond drying has also been investigated to determine the optimal drying conditions and dryer configuration design (Chilka and Ranade, 2019). Furthermore, CFD simulations have been used to compare drying conditions for corn under fair and overcast conditions in

solar dryers (Sanghi et al., 2018). The investigation of moisture content and temperature inside blanched and unbleached apricots was also conducted by using CFD simulations with experimental validation (Cârlescu et al., 2017). Thus, using CFD models to investigate drying conditions within drying chambers is essential. However, there are sparse studies on computer-aided modeling techniques for drying turmeric rhizomes in tray dryers. The primary objective of this project is to investigate the drying process of turmeric using this specific drying equipment by applying a CFD model to analyze the velocity, temperature, and humidity distribution of moist air. This analysis aims to evaluate the suitable conditions for turmeric drying.

## 2. Methodology

### 2.1 Experimental setup

The turmeric drying process was conducted using a Computer Controlled Tray Drier at Ho Chi Minh City University of Technology – Vietnam National University. 100 g of turmeric rhizomes were sliced into 2 mm thicknesses and placed on a tray with 128 x 215 mm dimensions inside a drying chamber measuring 1000 x 320 x 320 mm. The process used a drying agent at 50 °C and was repeated until the material mass stabilized, which was recorded three times before stopping the test. The weight, dry bulb temperature, and wet bulb temperature were recorded every minute.



Figure 1: (a) Computer Controlled Tray Drier and turmeric rhizomes; (b) before; (c) after drying process

### 2.2 Model Development and analysis

#### 2.2.1 Geometric modelling and grid generation

Figure 2 demonstrates the computational domain of the tray drier, including its physical model and meshing. The drying agent enters through the inlet, with its flow direction controlled by baffles. It then passes through the turmeric rhizomes tray before exiting the chamber. The geometry was discretized using the poly-hex core meshing method, resulting in 1,094,258 cells. The choice of mesh size was dependent on the accuracy requirements and the computational resources available. Due to computational equipment limitations, the mesh size in this study was optimized to use the minimum number of elements necessary to achieve the recommended mesh quality. Consequently, the minimum orthogonal quality was measured at 0.18, and the maximum skewness was 0.26, which meets acceptable mesh quality criteria (Adam et al., 2020).

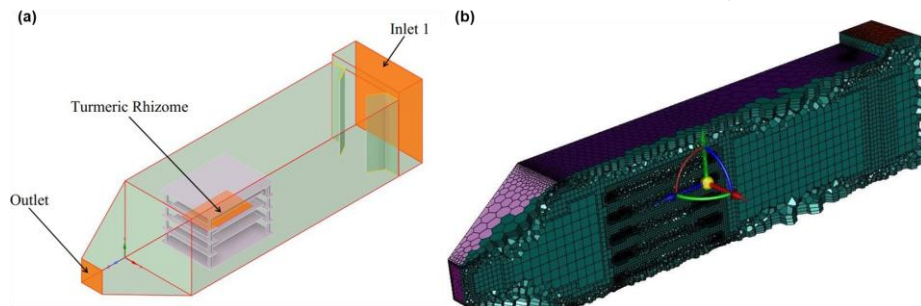


Figure 2: (a) The physical model and; (b) the grid domain of the tray drier

### 2.2.2 Turbulent model

The airflow within the drying chamber is expected to exhibit turbulent characteristics due to high flow rates, changes in surface area throughout the chamber, and heat transfer interaction within the flow field. The standard  $k$ - $\epsilon$  turbulence model was employed to model this turbulence, integrating transport equations for turbulent kinetic energy ( $k$ ) and its dissipation rate ( $\epsilon$ ). Additionally, the density was treated as a constant value in all equations by applying the Boussinesq model (Chilka and Ranade, 2019).

### 2.2.3 Species transport

The airflow in this research consisted of a combination of dry air and water vapor. The drying agent passing through the turmeric tray was considered moving through a porous zone. The porous area representing the dried material was used to model the moisture transfer process. The chemical components were preserved using the convective diffusion equation available in ANSYS Fluent. The local mass fraction of each species ( $Y_i$ ) was predicted by solving the corresponding equation for each substance in the mixture.

### 2.2.4 Boundary condition

The numerical solution of the model depends on the boundary conditions' values for fluid flow. The operating conditions and boundary conditions are provided in Table 1 and Table 2.

Table 1: Operating conditions

The operating conditions	Governing Equations
Solver	3D simulation Implicit formulation Absolute velocity formulation Transient state analysis
Energy equation	Activated
Viscous model	Standard $k$ - $\epsilon$ turbulence model
Species	Diffusion Energy Source

Table 2: Boundary condition

Boundary condition	Material	Parameter	Value	Unit
Inlet	Moist Air	Velocity	0.8571	[m/s]
		Temperature	50	[°C]
		Mass fraction of H <sub>2</sub> O	0.0521	
Outlet	Moist Air	Pressure	1	[atm]
		Temperature	47.7	[°C]

## 3. Results and discussion

### 3.1 Validation with the experimental results

Figure 3 compares the simulation and experimental results of the vaporization rate over 8,000 seconds. The experimental results show that the drying process can be divided into three stages based on the moisture evaporation rate. In the first 93 seconds, the material heats up quickly, leading to the highest rate of moisture evaporation, known as the material heating period. This rate then drops significantly until 2,730 seconds, during the constant rate drying period. Finally, the turmeric material evaporates at a slightly lower rate until it stabilizes, marking the drying period at a falling rate.

Based on these data, a drying curve was established to illustrate the vaporization rate of the turmeric material. This curve was modeled in ANSYS Fluent using three equations to represent the three stages of the drying process. The model showed a strong correlation between the simulation and experimental data, validating the accuracy of the simulation with the least square regression values of 1, 0.99, and 0.97 for each stage.

Figure 4 illustrates the locations where the temperatures in the chamber were recorded and compares the simulation and experimental results. Overall, the simulation shows a nearly constant temperature at both locations, around 50 °C before and 46.5 °C after drying. In contrast, the experimental results show some fluctuation, ranging from 49 °C to 50 °C before drying and from 47 °C to 47.5 °C after drying. Despite these fluctuations, the maximum temperature difference is only about 1 °C, resulting in a change of 1.7 % to 2.3 %. Therefore, there is no significant distinction between the simulated and experimental values.

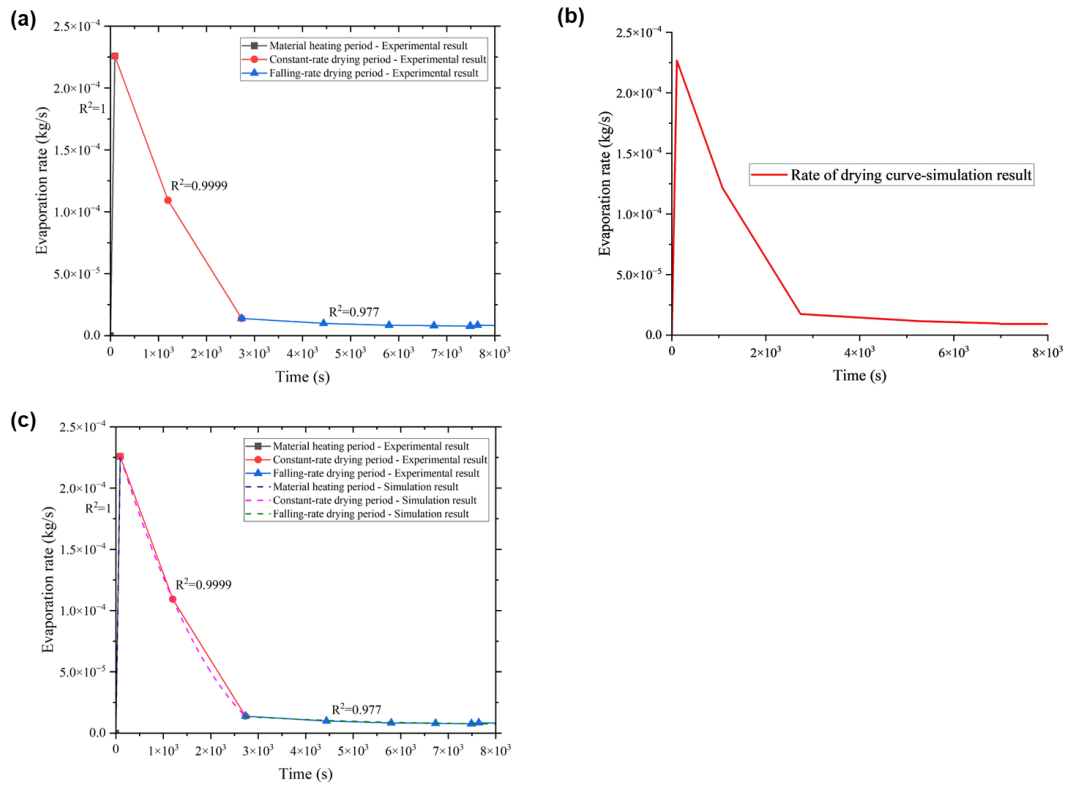


Figure 3: The (a) experimental; (b) simulation; and (c) validation of the evaporation rate of turmeric rhizome

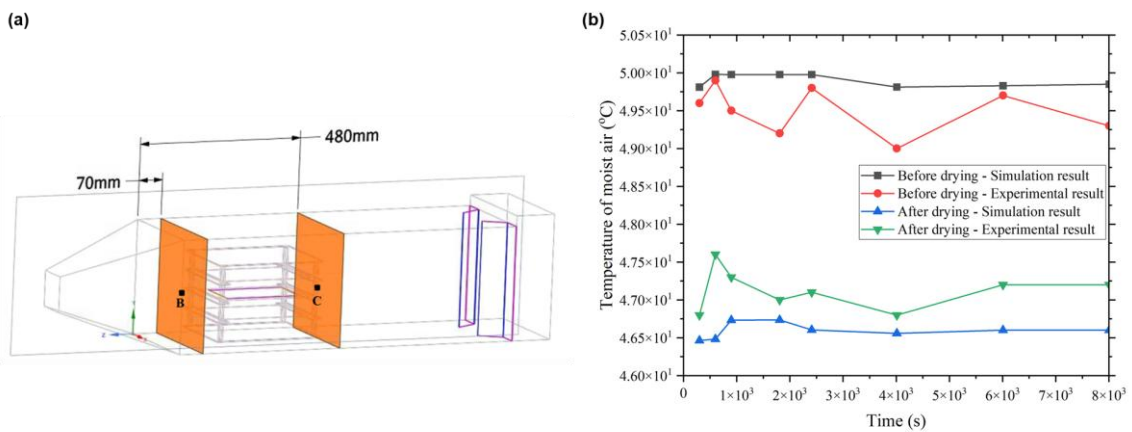


Figure 4: (a) The location to take the temperature before and after drying; (b) The temperature comparison between the simulation and experimental results

### 3.2 Temperature profile inside the drying chamber

Figure 5 shows the temperature distribution within the drying chamber at the plane  $x = 0.16$  m, located in the middle of the chamber. Overall, the temperature distribution remained relatively consistent over time. The drying medium's temperature is maintained at a constant inlet temperature of 323.15 K (50 °C) throughout the tray dryer until it reaches the sample. Heat exchange occurs as the hot air encounters the drying material, initially at room temperature (27 °C). The hot air, capable of holding more moisture than the moist air, extracts moisture from the sample, causing its temperature to decrease to 319.75 K (46.6 °C) by the end of the tray dryer. In the

first 1800 seconds, the temperature changes at the material covered a larger zone due to the higher evaporation rate. However, the overall change in this rate was insignificant.

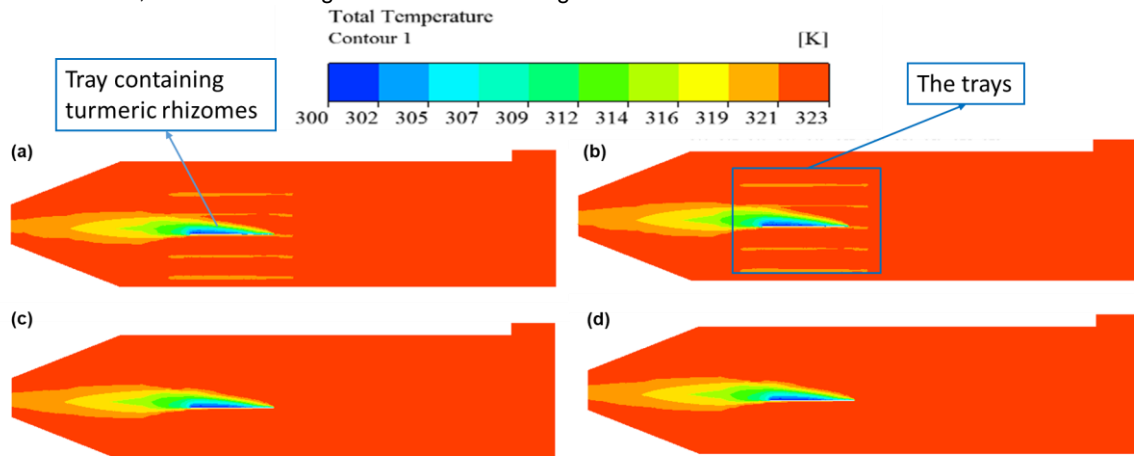


Figure 5: The temperature profile at (a) 300 s; (b) 1,800 s; (c) 6,000 s; and (d) 8,000 s

### 3.3 Moisture distribution with the drying chamber

The moisture profile is a crucial aspect to investigate in the drying process. One of the key factors affecting moisture distribution is the velocity of the drying air within the drying chamber, which directs the water evaporation process. Figure 6 illustrates the velocity vectors within the dryer. Initially, the drying agent passed through a pair of baffles, creating higher velocities in the middle and directing the airflow through the center of the tray where the material was placed, thus enhancing evaporation. At the end of the drying chamber, an increase in velocity, at around 10 m/s, is observed due to the change in surface area at the outlet.

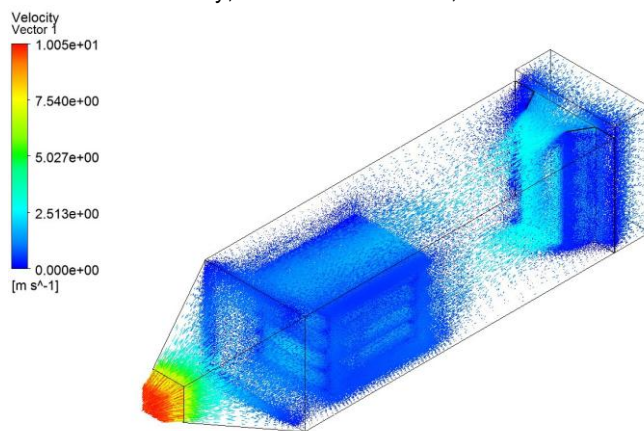


Figure 6: The velocity profile of the tray drier

Figure 7 shows the changes in the water mass fraction at  $z = -0.15$  m over the drying period. Overall, the mass fraction of water decreases over time, consistent with the drying curve characteristics shown in Figure 3. Initially, during the first period, the rate of evaporation of the drying material rapidly reaches its maximum value of 0.1021 kg water vapor/kg moist air. Subsequently, the amount of moisture evaporated gradually decreases and stabilizes at approximately 0.0921 kg water vapor/kg moist air. This decrease in the evaporation rate can be attributed to the diminishing moisture content in the dried material over time. This trend is further supported by the experimental findings, which show that the evaporation rate of turmeric initially reaches its peak, leading to a significant increase in the mass fraction of water vapor in the wet air.



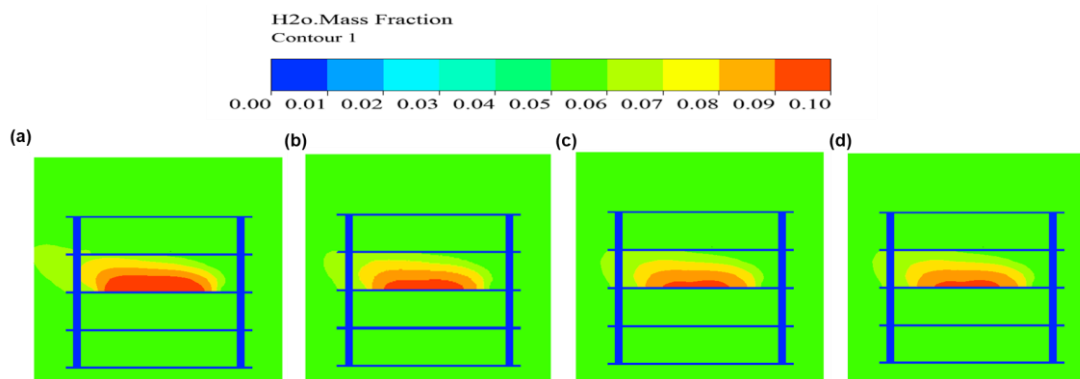


Figure 7: Mass fraction of  $H_2O$  at the contour  $z = -0.15$  m at (A) 300 s; (B) 1,800 s; (C) 6,000 s; (D) 8,000 s

#### 4. Conclusion

In this research, the tray dryer was simulated in three-dimensional geometry using ANSYS Fluent, accurately replicating the actual tray dryer's dimensions. The mesh model, consisting of over 1,000,000 poly-hex core cells, met standard quality criteria. The numerical results were validated against experimental measurements of turmeric's evaporation rate, accurately capturing the three drying process periods, including material heating, constant-rate drying, and falling-rate drying, with strong correlations indicated by  $R^2$  values of 1, 0.99, and 0.97. Temperature comparisons before and after entering the tray zone showed minimal errors of approximately 1.7 % and 2.3 %. Airflow velocity was observed to start at 0.85 m/s at the entrance, increase to 2.5 m/s after passing through baffles, and drop to 0.5 m/s in the solid tray zone, with a peak velocity of 9.6 m/s at the exit. Moisture distribution ranged from 0.0921 to 0.1021 kg water vapor/kg moist air within the drying material zone. These results confirm the model's accuracy and effectiveness in simulating the drying process. Future research can utilize CFD simulations to explore various drying conditions to determine the optimal process parameters, and investigate the moisture content inside turmeric rhizomes to enhance drying efficiency.

#### References

- Adam N.M., Attia O.H., Al-Sulttani A.O., Mahmood H.A., As'array A., Rezali K.A.M., 2020, Numerical analysis for solar panel subjected with an external force to overcome adhesive force in desert areas, *CFD Letters*, 12(9), 60–75.
- Cârlescu P. M., Arsenoiaia V., Roșca R., Tenu I., 2017, CFD simulation of heat and mass transfer during apricots drying, *LWT - Food and Science Technology*, 85, 479–486.
- Chilka A. G., Ranade V. V., 2019, CFD modelling of almond drying in a tray dryer, *Canadian Journal of Chemical Engineering*, 97(2), 560–572.
- Duong Y.H.P., Vo N.T., Le P.T.K., Tran V.T., 2021, Three-Dimensional Simulation of Solar Greenhouse Dryer, *Chemical Engineering Transactions*, 83, 211–216.
- Getahun E., Delele M.A., Gabbiye N., Fanta S.W., Demissie P., Vanierschot M., 2021, Importance of integrated CFD and product quality modeling of solar dryers for fruits and vegetables: A review, *Solar Energy*, 220, 88–110.
- Misha S., Mat S., Ruslan M. H., Sopian K., Salleh E., 2013, The Prediction of Drying Uniformity in Tray Dryer System using CFD Simulation, *International Journal of Machine Learning and Computing*, 3(5), 419–423.
- Nadew T.T., Tegenaw P.D., Tedila T.S., 2023, Mathematical-Based CFD Modelling and Simulation of Mushroom Drying in Tray Dryer, *Modelling and Simulation in Engineering*, 2023, 1-19.
- Nguyen H.T., Trinh Q.P., Nguyen T.D., Bert W., 2020, First report of *Rotylenchulus reniformis* infecting turmeric in Vietnam and consequent damage, *Journal of Nematology*, 52, 1–5.
- Sanghi A., Ambrose R.P.K., Maier D., 2018, CFD simulation of corn drying in a natural convection solar dryer, *Drying Technology*, 36(7), 859–870.